615857

AIAA 2002-4617
Mars Smart Lander Parachute Simulation Model

Eric M. Queen and Ben Raiszadeh

NASA Langley Research Center
Hampton, VA 23681

AIAA Atmospheric Flight Mechanics Conference & Exhibit

August 5-8, 2002
Monterey, California

AIAA 2001-4617

MARS SMART LANDER PARACHUTE SIMULATION MODEL

Eric M. Queen* and Ben Raiszadeh†
NASA Langley Research Center, Hampton, VA-23681.

Abstract

A multi-body flight simulation for the Mars Smart Lander has been developed that includes six degree-of-freedom rigid-body models for both the supersonically-deployed and subsonically-deployed parachutes. This simulation is designed to be incorporated into a larger simulation of the entire entry, descent and landing (EDL) sequence. The complete end-to-end simulation will provide attitude history predictions of all bodies throughout the flight as well as loads on each of the connecting lines. Other issues such as recontact with jettisoned elements (heat shield, back shield, parachute mortar covers, etc.), design of parachute and attachment points, and desirable line properties can also be addressed readily using this simulation.

Introduction

A multi-body flight simulation for the Mars Smart Lander has been developed that includes high fidelity models for both the supersonically-deployed and subsonically-deployed parachutes. While parachute models are necessary for simulation of all Mars Landers, the Mars Smart Lander will have a capability, namely active, autonomous, on-board Hazard Detection and Avoidance (HDA) that makes the inclusion of these models even more imperative. None of the Mars Landers to date have had an active on-board HDA system. This HDA function for these earlier landers has been served by a combination of restricting the landing to "safe" sites as judged by the Mars Project Office and by "robust" lander design. Restriction of landing site places limitations on the scientific objectives that can be achieved, while robust lander design commits a large amount of mass to components which provide no added value to the mission. The Mars Smart Lander will include an active HDA designed to insure a safe touchdown even in hazardous terrain, thus allowing safe landings in areas that would be considered too dangerous for missions to date. The hazards to be avoided include rocks, craters, and large sloping terrain. The HDA system is currently envisioned to be composed of lidar and radar elements that map the local terrain and determine the location of safe landing zones. The information gathered from the sensors would be provided to the on-board guidance algorithm, which would modify the target point to avoid the detected hazards. To accurately model this HDA capability requires an accurate end-to-end simulation of the entire entry, descent and landing (EDL) sequence. Flight simulation of spacecraft with parachutes is mathematically complicated and not easily characterized with traditional approaches. It involves multiple bodies, some of which are very flexible, flying in close proximity with significant interaction effects. In previous Mars Lander missions, a separate simulation was developed for the parachute portion of flight, independent of the other portions of the EDL, because the dynamics are so different from the rest of the entry. This was the approach followed for Mars Pathfinder and Mars Polar Lander. The Mars Pathfinder and Mars Polar Lander parachute

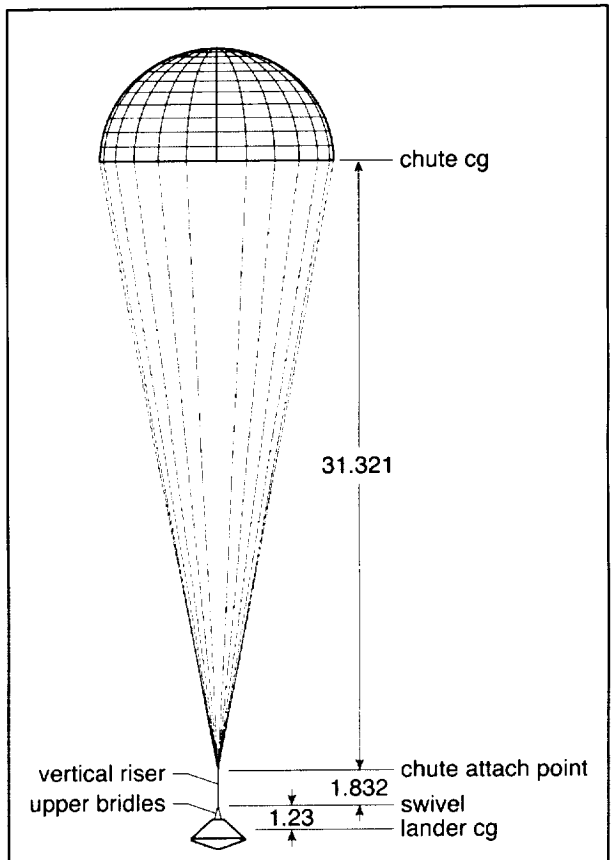

Figure 1: Mars Smart Lander entry configura-

simulations were done in ADAMS [1]. ADAMS is a commercial-off-the-shelf program that is used to simulate the motions of multiple rigid bodies. ADAMS was tailored for parachute simulation for Mars Pathfinder, and used by the Mars Polar Lander project. However, this exclusive use of ADAMS for modeling the spacecraft while on the parachutes is not desirable for the Mars Smart Lander, as the results from the HDA system interacts with the guidance commands. Thus it was decided to develop an End-to-End Mars Smart Lander simulation that included parachute dynamics.

The goal of this work is to develop a multibody simulation of flight under a parachute that can easily be incorporated into a larger simulation of the entire entry, descent and landing (EDL) sequence. In this work the parachute is treated as rigid body, with the interaction forces between the parachute and other rigid bodies included. A similar treatment was used to simulate Viking drop-test flights [2,3]. This will provide the capability to create an end-to-end simulation from the last trajectory correction maneuver before atmospheric entry down to touchdown. This simulation will provide the attitude history predictions of all bodies throughout the flight, which is required to model the performance of the HDA subsystem. Other issues such as recontact with jettisoned elements (heat shield, back shield, parachute mortar covers, etc.), design of parachute and attachment points, and desirable line properties can also be addressed readily using this simulation.

Mission Description

The 2009 Smart Lander mission to Mars described in this report performs a direct entry at Mars. The vehicle slows itself through atmospheric drag until about Mach 2.2, at which point a supersonic parachute similar to that used for Viking and Pathfinder is deployed. The geometry of the lander with a supersonic parachute deployed is shown in figure 1. When the vehicle is further slowed to Mach 0.8, a subsonic parachute is opened. At the time the subsonic parachute is opened, the supersonic parachute is jettisoned, taking the vehicle backshell with it. After the subsonic parachute is fully deployed, the lander heatshield is jettisoned. The lander descends until its altitude is between 800 and 500 meters. At an altitude determined by the onboard guidance, the lander separates from the subsonic parachute and descends to the surface under power of its main descent engines.

Approach

The underlying simulation used for the Mars Smart Lander is the Program to Optimize Simulated Trajectories II (POST II). POST II is the latest major upgrade to POST [4]. POST was originally developed for the Space Shuttle program to optimize ascent and entry trajectories. Over the years it has been upgraded and improved to include many new capabilities. POST II relies on most of the technical elements established by POST, but the executive structure has been reworked to take advantage of today's faster computers. The new executive routines allow POST II to simulate multiple bodies simultaneously, and to mix three degree of freedom (3DOF) bodies with six degree of freedom (6DOF) bodies in a single simulation. The multiple body capability allows POST II to simulate parachutes. This is done as follows. The lines connecting the spacecraft and the parachutes are modeled as massless spring-dampers. The springs can be attached at any point on the body. No moments are applied except those due to force application away from the center of mass. Each line connects an attachment point on one body to an attachment point on another body and provides a tension-only force. When the lines are stretched, tension in the lines is determined as a function of strain and strain rate. The spring force may be linearly proportional to strain and the damping force is proportional to the strain rate or may be a more complicated nonlinear relationship. In the nonlinear technique, the line forces are not linearly proportional to the strain and the strain rate. The spring stiffness and damping coefficients are provided by the user as functions of strain and strain rate. In this nonlinear model, the coefficients tend to be smaller at lower strains. Each of the spring-damper lines has an unstretched length and if the separation distance between the two attach-points is less than the unstretched length, the line tension is zero.

For the results shown in this report, damping and stiffness were both assumed to be linear. For the vertical risers, both subsonic and supersonic, the stiffness used was 60000 N/m while for the bridle lines the stiffness was 47000 N/m. The damping in the vertical risers was 600 N/m/sec, while the damping in the bridles was 470 N/m/sec.

In order to accurately target a selected site and to insure that the parachute is deployed within its structural limits, onboard guidance and control systems are used. These guidance and control systems were modeled in the simulation. The guidance system used is one based on a calculus of variations approach and is similar to the Apollo Earth-Return Terminal guidance. The guidance algorithm is described in detail in [5]. The control system used is a phase-plane controller with each of the three axes controlled independently. The phase-plane controller is described in [6].

Model Validation

In order to validate the multibody capability of POST II with interacting forces, a series of more than 35 tests of increasing complexity were performed. These tests were intended to prove that the POST II model is implemented correctly by evaluating its performance on problems that could be verified by other means. The test cases started with a simple vertical drop from rest of the fully deployed parachute and entry body and gradually increased in complexity to include parachute opening, non-zero initial conditions, line deployment and other effects. The POST II model was compared to both MATLAB-based and ADAMS-based multi-degree-of-freedom simulations. In each case the agreement between the simulations was excellent. These tests have validated the general parachute model within POST II. Some of the validation work is reported more fully in [7]

Results

After completion of the validation phase, the specific parachute configuration of the Mars Smart Lander has been incorporated into the simulation. This case begins 60 seconds prior to atmospheric entry. Atmospheric entry is assumed to occur at a radius of 3522.2 km. The initial velocity is 5.65 km/s and the initial flight path angle is –15.73 degrees, leading to an entry flight path of –12.13 degrees. When the vehicle is slowed to Mach 2.2 (approximately 480 m/s), the parachute is ejected from the back of the spacecraft by a mortar with a velocity relative to the spacecraft of 36.576 m/s. The parachute is held by a bag (assumed massless) until the

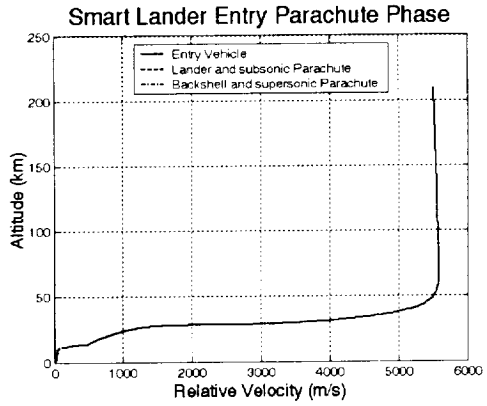

Figure 2: Mars Smart Lander entry trajectory

lines connecting the parachute to the vehicle become taut, at which point, the bag is discarded and the parachute begins to inflate. It is assumed that the inflation profile is a function of time only. Figure 2 shows the entry altitude as a function of velocity and figure 3

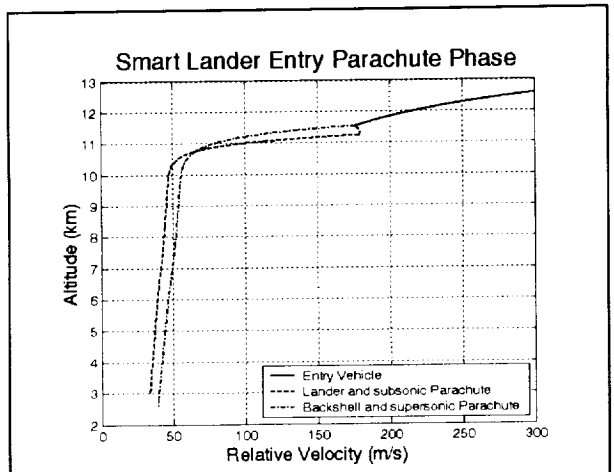

Figure 3: Mars Smart Lander entry trajectory (Detail)

shows a detail of the final part of the altitude velocity curve. The subsonic parachute is deployed at Mach 0.8 (about 200 m/s) and the backshell and supersonic parachute separate from the lander and subsonic parachute. The backshell impacts the ground at about 40 m/s. The current simulation ends when the lander reaches 500 m AGL (3000m above the reference ellipsoid), as that is the lowest altitude at which the guidance algorithm will command separation from the subsonic parachute. Figure 4 shows the line tension for 4 of the connecting lines as a function of time. The supersonic parachute deploys about 388 seconds after atmospheric entry

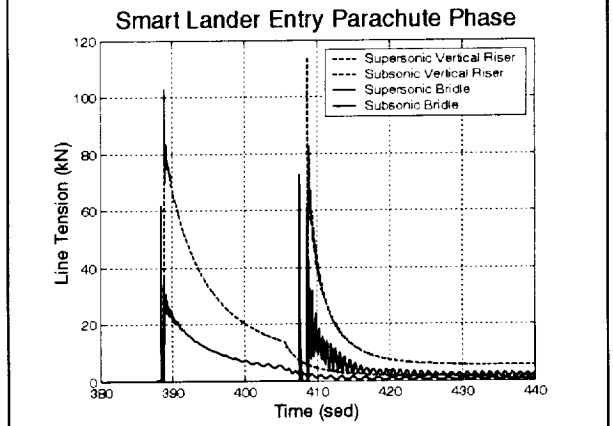

Figure 4: Mars Smart Lander entry Parachute line Loads

while the subsonic parachute deploys about 409 seconds after entry. In each case the bridle loads are about 1/3 of the vertical riser loads, since there are three bri-

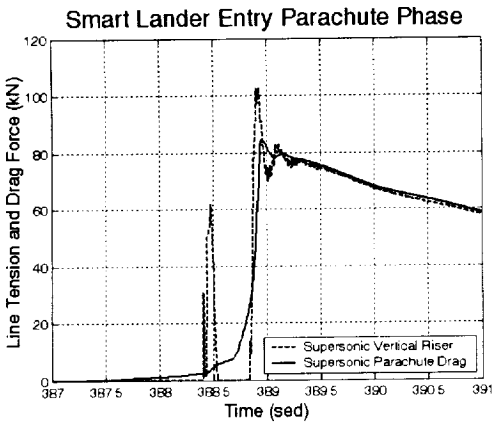

Figure 5: Parachute line Loads compared to Drag force

dle lines in parallel for each of the vertical risers.

Figure 5 is a detail from figure 4 showing the initial loads on the supersonic parachute vertical riser line. Also shown is the drag on the supersonic parachute. The force on the vertical riser is the summation of the parachute drag force and the inertial forces. In this figure, the first peak (snatch load) is due primarily to inertial forces, as the ejected parachute reaches the end of

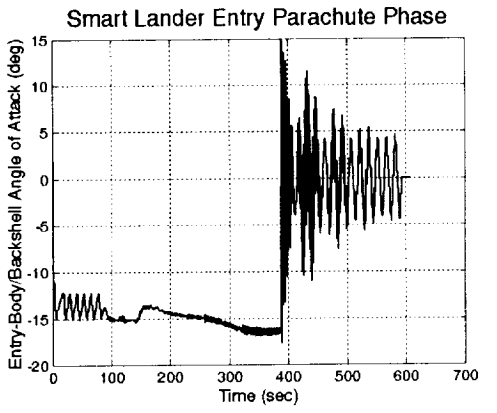

Figure 6: Entry Vehicle/Backshell Angle of Attack

its line and rebounds, while the second, larger, peak is due primarily to drag on the parachute (opening load). After the second peak, the drag force reduces as the vehicle slows and the dynamic pressure drops off.

The angle of attack of the entry vehicle and later the backshell is shown in figure 6. During the entry portion of flight before the parachute is deployed, the angle of

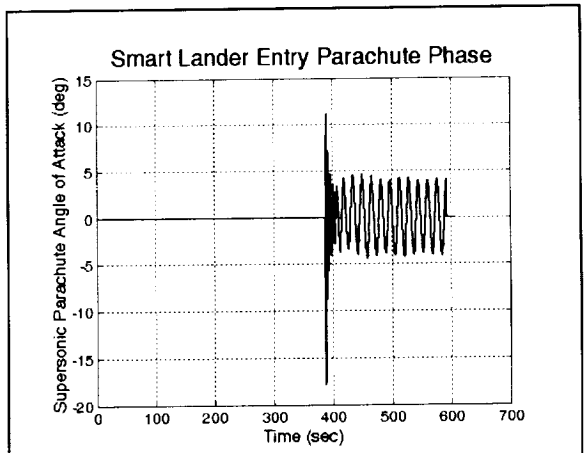

Figure 7: Supersonic Parachute Angle of Attack

attack is constrained by the control system to remain near its trim angle of attack of about –15 degrees. After the parachute is opened the aerodynamics of the vehicle-parachute combination is dominated by the parachute. The angle of attack of the entry body/backshell is

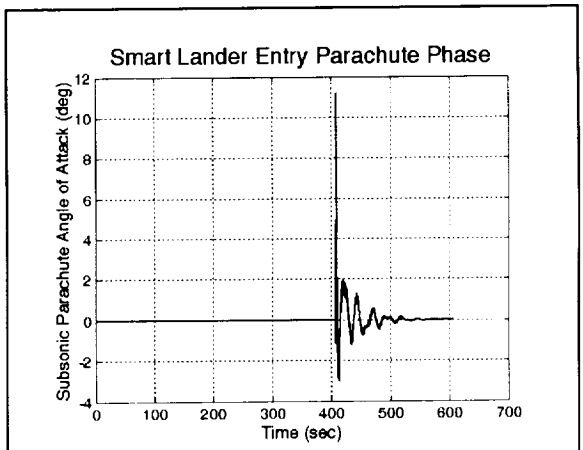

Figure 8: Subsonic Parachute Angle of Attack

determined by the dynamics of the parachute-lander system. Figures 7 and 8 shows the angle of attack for the two parachutes. The supersonic parachute is seen to oscillate with an amplitude of about five degrees while the subsonic parachute quickly settles to a constant angle of attack. The oscillation of the supersonic parachute may be due to the smaller load it carries. After about 409 seconds the supersonic parachute only sup-

ports the backshell.

The distance between the Lander and the Backshell is

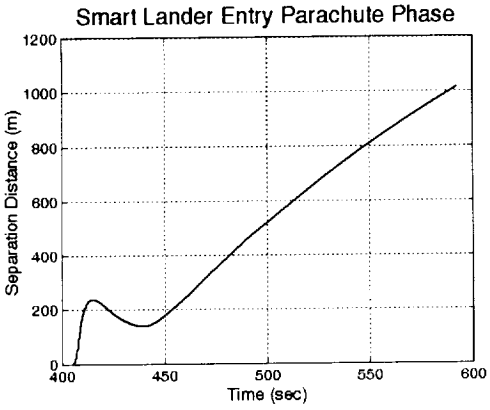

Figure 9: Separation distance between Lander and Backshell

shown in figure 9. This shows that the two bodies separate, move toward each other and separate again more permanently. In this case recontact between the pieces was not an issue, but a more detailed analysis is recommended to address all recontact issues.

Conclusions

A multiple rigid-body parachute simulation model for the Mars Smart Lander entry phase has been developed. The model includes dynamics caused by interacting lines in a way that is easily incorporated into an end-to-end simulation of the entry phase. The model has been used to examine a nominal trajectory from entry until the lander drops from the subsonic parachute. The loads on each of the lines connecting the various bodies were calculated and found to be less than 120 kN for each line. It was seen that the line loads closely followed the parachute drag force, as expected. The main difference between the line load and the parachute drag was due to inertial loads as the parachute was deployed. The attitude of each body was computed and seen to be reasonable for this vehicle. Finally, the separation distance between the lander and backshell was computed and it was determined that, for this case, recontact was not an issue, but further analysis is needed.

References

1. Kenneth S. Smith, Chia-Yen Peng, Ali Behboud, *Multibody Dynamic Simulation of Mars Pathfinder Entry, Descent and Landing*, JPL D-13298, April 1995.

2. Theodore A.Talay, *Parachute-Deployment-Parameter Identification Based on an Analytical Simulation of Viking BLDT AV-4*, NASA TN D-7678, August 1974.

3. Renjith R. Kumar, Juan R. Cruz, *Mars Airplane Package (MAP), Parachute and Aeroshell Multibody Dynamics Simulation: Comparison with Viking BLDT AV-4 Test Results and Sensitivity Analysis*, Document 0804-04-01A, May 2000.

4. *Program to Optimize Simulated Trajectories: Volume II, Utilization Manual*, prepared by: R.W. Powell, S.A. Striepe, P.N. Desai, P.V. Tartabini, E.M. Queen; NASA Langley Research Center, and by: G.L. Brauer, D.E. Cornick, D.W. Olson, F.M. Petersen, R. Stevenson, M.C. Engel, S.M. Marsh; Lockheed Martin Corporation. Version 1.1.1.G, May 2000.

5. G. Carman, D. Ives, and D. Geller, *Apollo-Derived Mars Precision Lander Guidance*, AIAA 98-4570, AIAA Atmospheric Flight Mechanics Conference, August 10-12, 1998, Boston, Ma.

6. P. Calhoun and E. Queen, *An Entry Vehicle Control System Design for the Mars Smart Lander*, AIAA Atmospheric Flight Mechanics Conference , August 5-8, 2002, AIAA 2002-4504

7. B. Raiszadeh, and E. Queen, *Partial Validation of Multibody Parachute model in POST II*, NASA TM-2002-211634

8. E. G. Ewing, H. W. Bixby, T W. Knacke, *Recovery Systems Design Guide*, AFFDL-TR-78-151, December 1978.